Simple iterative receivers for MIMO LP-OFDM systems

Pierre-Jean BOUVET*, Maryline HÉLARD**, Vincent LE NIR***

Abstract

In this paper, LP-OFDM is combined with different MIMO schemes in order to improve performance in terms of diversity gain and to exploit capacity brought by the MIMO channel. The original contribution is the development of a generic iterative receiver designed for LP MIMO transmission able to work whatever the antenna configuration and the spatial coding scheme. By using a global MMSE criterion, interference terms coming from space-time coding and linear precoding are jointly treated leading to a very good trade-off between performance and complexity compared to trellis based detectors particularly for high order modulations, high number of antennas and/or large size of precoding matrices.

Key words: Radiocommunication, Space diversity, OFDM, Jeu signal, Itération, Transformation linéaire, Récepteur, Simulation.

RÉCEPTEUR ITÉRATIF SIMPLE POUR SYSTÈMES MIMO-OFDM ET À PRÉCODAGE LINÉAIRE

Résumé

Dans cet article, le précodage linéaire est associé à différents schémas multi-antennes dans un contexte OFDM afin d'améliorer les performances en termes d'exploitation de diversité et de capacité offertes par les canaux multi-antennes. La contribution originale est de proposer un récepteur itératif générique pour schémas LP-MIMO pouvant s'adapter à n'importe quelle configuration d'antennes et de codage spatio-temporel. Les termes d'interférence qui proviennent du précodage linéaire et du codage spatio-temporel sont traités conjointement en utilisant un critère de minimisation de l'erreur quadratique moyenne globale. Le récepteur obtenu permet d'obtenir un très bon compromis entre les performances et la complexité de mise en œuvre comparé à des détecteurs à base de treillis en particulier pour les modulations à nombre d'états élevé, des systèmes à plusieurs antennes d'émission et de réception et/ou des grandes tailles de matrice de précodage.

Mots clés : Radiocommunication, Diversité spatiale, OFDM, Constellation signal, Itération, Linear transformation, Receiver, Simulation.

* P.J. Bouvet is now with Philips Semiconductors, Home Innovation Center (HIC) – 2, rue de la girafe, 14079 Caen cedex 5, France; pierre-jean.bouvet@philips.com
** France Telecom R&D, RESA/BWA Laboratory – 4, rue du Clos Courtel, BP 91226, 35512 Cesson Sévigné Cedex, France; maryline.helard@francetelecom.com
*** V. Le Nir is now with the Katholieke Universiteit Leuven, Departement Elektrotechniek (ESAT) – Kasteelpark Arenberg 10 B-3001 Leuven-Heverlee, Belgium; Vincent.LeNir@esat.kuleuven.ac.be

Most of results presented in this paper have been obtained during the PhD thesis of P.-J. Bouvet and V. Le Nir at France Telecom R&D.

Contents

I. INTRODUCTION

Increasing the number of antennas is a prospective solution to improve performance of wireless transmissions. The spectral efficiency of a multiple-input multiple-output (MIMO) system is known to be much higher than a conventional single antenna link. In fact, under the assumption of a full rank multi-antenna channel, capacity of a MIMO system has been demonstrated to grow linearly with the minimum of transmit and receive antennas [1, 2]. By assuming channel state information (CSI) at the receive side (well adapted to radio-mobile transmission), the capacity and diversity gains of multiple antenna systems are usually exploited by using either spatial multiplexing transmission scheme or space-time block coding (STBC) architecture [3, 4, 5, 6].

Diversity techniques are traditionally used to combat channel fading due to multi-path propagation. By carrying the same information through different paths, the reception is achieved with more reliability. Initially introduced for single input single output (SISO) transmission, linear precoding (LP), also called constellation rotation, is a promising technique that exploits channel diversity without knowledge at the transmit side and without bandwidth expansion [7]. By combining LP with orthogonal frequency division multiplex (OFDM), the so-called LP-OFDM scheme was demonstrated to efficiently exploit time and frequency diversities [8, 9]. In case of multi-antenna transmission, each independent sub-link can be viewed as a new source of diversity. In order to take benefit from this spatial diversity, linear precoding principle has recently been extended to MIMO system leading to new space-time coding structures [10, 11, 12, 13, 14].

At the receive side, the detection algorithm has to deal with both effects of multi-antenna transmission and/or linear precoding. In [11, 12], owing to a particular combination of linear precoding with orthogonal STBC leading to low interference terms, simple linear receiver provides very good performance for non coded transmission. In the presence of channel coding, the optimal receiver consists of a maximum likelihood (ML) detector based on super-trellis taking into account the structures of the space-time coding, linear precoding, interleaving and channel coding. For complexity reason, such ideal receiver could not be reasonably implemented in a chip.

By extending the turbo-detection principle initially introduced in the field of equalization for frequency selective channels in single-carrier transmission [15], efficient iterative receivers have been proposed for LP-OFDM systems [16] or MIMO-OFDM systems [17]. Particularly, in [18] the authors derived a receiver performing jointly MIMO detection, linear deprecoding, and channel decoding in an iterative loop. However all these iterative receivers have an equa-

lization stage based on trellis-search algorithms leading to an overall complexity growing exponentially with the precoding size, the number of antennas and the modulation order. In order to deal with this high complexity, simpler solutions have been recently proposed either for MIMO transmissions [19, 20, 21, 22] or for linear precoded SISO transmissions [23, 24]. These efficient algorithms are coming from filter-based turbo-equalization principle initially proposed in [25, 26, 27]. In [28], a low complexity iterative receiver has been extended to linear precoded MIMO transmission. However on the one hand space-time decoding and linear deprecoding are not jointly optimized and on the other hand the equalization stage is based on the matched filter approximation (see [29] for details). For all these reasons, such solution leads to sub-optimal performance.

In this paper, LP-OFDM is combined with different MIMO schemes in order to improve performance in terms of diversity gain and to exploit capacity brought by the MIMO channel. The original contribution is the development of a generic iterative receiver designed for LP MIMO transmission able to work whatever the antenna configuration. By using a global minimum mean square error (MMSE) criterion, interference terms coming from space-time coding and linear precoding are jointly treated leading to a very good trade-off between performance and complexity compared to trellis based detectors particularly for high order modulations, high number of antennas and large size of precoding matrices.

The paper is organized as follows. In part II, all stages of the transmitter are detailed: linear precoding, MIMO systems studied in this paper i.e. spatial multiplexing and orthogonal STBC and finally the MIMO LP-OFDM transmitter. In the third part, two different types of non iterative receivers are presented: a maximum likelihood based one and a linear MMSE based one. Then, the iterative receiver is detailed. In part V, simulation results are provided for independent frequency non-selective Rayleigh channels per subcarrier and per antenna by considering SISO, STBC and spatial multiplexing schemes respectively. Conclusions are drawn in the last part.

Notations: bold lower (upper) case letters are used to denote vectors (matrices). Superscript $(.)^*$, $(.)^T$ and $(.)^H$ denote the complex conjugate, the matrix transpose and the conjugate transpose operators respectively. The operand $E[.]$ denotes the mathematical expectation.

II. SYSTEM MODEL

II.1. Linear precoding

The principle of linear precoding is to linearly combine L symbols of an information vector $\mathbf{x}$ with the help of a complex unitary matrix Θ_L of size $L \times L$ in order to bring diversity between each component of the resulting vector $\mathbf{s} = \Theta_L \mathbf{x}$. By using ML based receivers, authors of [7] show that L-order diversity can be achieved by that way. Moreover this diversity is brought without bandwidth expansion and without any channel knowledge at the transmit side. Since the multiplication by a unitary matrix keeps the Euclidean distance between constellation symbols unchanged and thus it does not alter performance when the channel is purely equal to additive white Gaussian noise (no fading), unitary matrices are

preferred for linear precoding. Usual precoding matrices are presented in Annex A that are Fourier, Vandermonde and complex Hadamard matrices. Extended study on precoding matrix optimization has been proposed in [30] under the assumption of ML decoding. In this paper, we choose a unitary precoding matrix based on Hadamard construction demonstrated to provide good performance with MMSE decoding when combined with the Alamouti code [11]:

(1)
$$\Theta_L = \sqrt{\frac{2}{L}} \begin{bmatrix} \Theta_{L/2} & \Theta_{L/2} \\ \Theta_{L/2} & -\Theta_{L/2} \end{bmatrix}$$

with
$$\Theta_2 = \frac{1}{2} \begin{bmatrix} -1-j & -1+j \\ 1+j & -1-j \end{bmatrix}$$

Figure 1 represents the constellation of the linear precoded Quadrature Phase Shift Keying (QPSK) symbols with the complex Hadamard matrix and $L = 4$. The use of complex Hadamard matrices leads to constellation with $(L+1)^2$ points. Figure 2 represents the density of probability of the real part of linearly precoded QPSK symbols with a Hadamard complex unitary matrix of size $L = 256$. We can see that the probability density of the resulting constellation approaches a discrete complex Gaussian density. Results not shown in this paper demonstrate that a similar density function is obtained whatever the choice of the precoding matrix if L is large enough. Shannon demonstrated in [31] that the channel capacity is optimum when the transmitted symbols follow a complex Gaussian law. Since linear precoding transforms modulation symbols into complex Gaussian symbols, the capacity of the resulting system is increased.

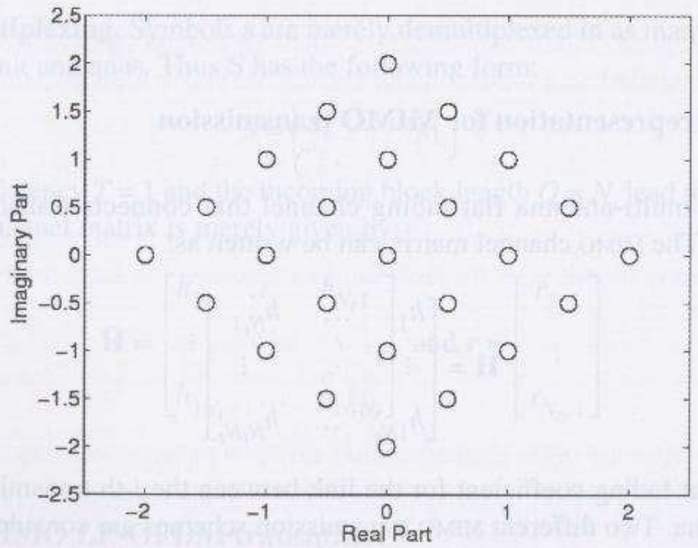

FIG. 1 – Transmitted constellation of linear precoded QPSK symbols for L = 4 with a complex Hadamard unitary matrix.

Constellation des symboles QPSK émis après précodage linéaire avec L = 4 et une matrice unitaire de type Hadamard complexe.

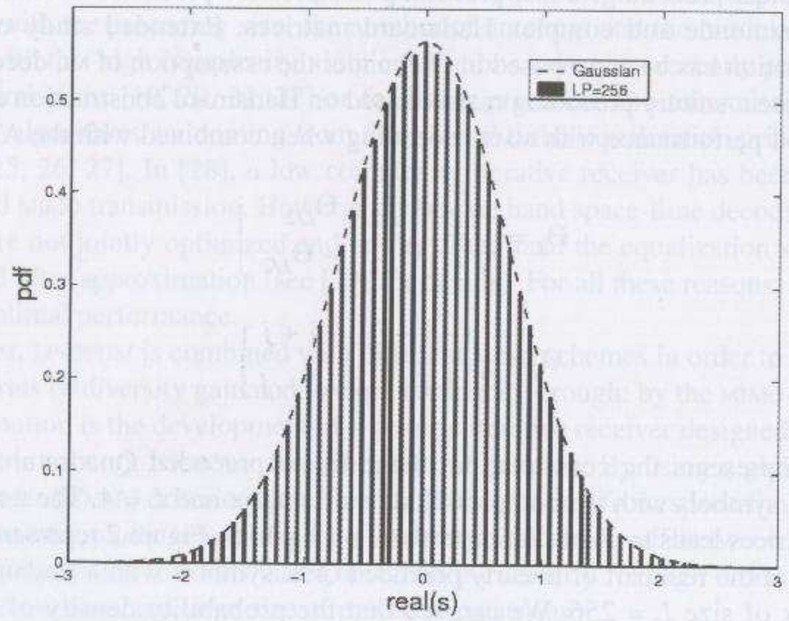

FIG. 2 – Distribution of real part of QPSK symbols precoded with the complex Hadamard unitary matrix with $L = 256$.

Fonction de densité de probabilité de la distribution de la partie réelle des symboles QPSK précodés avec une matrice unitaire de type Hadamard complexe avec L = 256.

II.2. Equivalent representation for MIMO transmission

Let assume a multi-antenna flat fading channel that connects transmit antennas and receive antennas. The MIMO channel matrix can be written as:

$$\mathbf{H} = \begin{bmatrix} h_{11} & \cdots & h_{N_t 1} \\ \vdots & \ddots & \vdots \\ h_{1N_r} & \cdots & h_{N_t N_r} \end{bmatrix} \quad (2)$$

where h_{ij} is the flat fading coefficient for the link between the i-th transmit antenna and the j-th receive antenna. Two different MIMO transmission schemes are considered in this paper: the STBC of Alamouti that provides high diversity performance by keeping a simple linear algorithm at the receive side [4] and a spatial multiplexing system that efficiently exploits the MIMO capacity [3].

The MIMO mapping represented by a coding matrix $\mathbf{S}$ of size $T \times N$ takes a block of Q incoming complex symbols s_k and sends the element (t, i) of $\mathbf{S}$, that can be either $\pm s_k$ or $\pm s_k^*$, to antenna i at sampling time tT_s where $1 \le k \le Q$ and T_s is the symbol duration. The

MIMO coding scheme is characterized by its latency T and its rate defined as $R_s = Q/T$. For the two MIMO techniques considered in this paper, an equivalent channel representation is introduced in order to take into account both space-time mapping and MIMO channel response. Let $\mathbf{s}$ the incoming block of length Q to be transmitted, an equivalent receive vector $\mathbf{r}$ of size $N_r T$ can be expressed as:

$$\mathbf{r} = \breve{\mathbf{H}}\mathbf{s} + \mathbf{n} \quad (3)$$

where $\breve{\mathbf{H}}$ of size $N_r T \times Q$ is the equivalent MIMO channel and $\mathbf{n}$ an equivalent noise vector [6].

- **Alamouti STBC scheme**. Let first consider the Alamouti scheme for a MIMO channel with $N_t = 2$ and $N_r = 1$. The coding matrix is:

$$\mathbf{s} = \begin{bmatrix} s_1 & s_1 \\ -s_2^* & s_1^* \end{bmatrix} \quad (4)$$

The STBC is applied to a block of $Q = 2$ incoming symbols whilst the channel is assumed to be constant over $T = 2$ symbol durations. The equivalent representation of the Alamouti STBC is therefore:

$$\breve{\mathbf{H}} = \begin{bmatrix} h_{11} & h_{21} \\ -h_{21}^* & h_{11}^* \end{bmatrix} \text{ and } \mathbf{r} = \begin{bmatrix} r_{1,1} \\ -r_{1,2}^* \end{bmatrix}. \quad (5)$$

where h_{11} and h_{21} are assumed to be constant over two symbol durations whereas $r_{j,t}$ is the receive symbol on antenna j at sampling time tT_s. The rate of the Alamouti scheme is therefore equal to $R_s = 1$.

- **Spatial multiplexing**. Symbols $\mathbf{s}$ are merely demultiplexed in as many streams as number of transmit antennas. Thus $\mathbf{S}$ has the following form:

$$\mathbf{s} = \begin{bmatrix} s_1 & \cdots & s_{N_1} \end{bmatrix} \quad (6)$$

The resulting latency $T = 1$ and the incoming block length $Q = N_t$ lead to a rate of $R_S = N_t$. The equivalent channel matrix is merely given by:

$$\breve{\mathbf{H}} = \begin{bmatrix} h_{11} & \cdots & h_{N_t 1} \\ \vdots & \ddots & \vdots \\ h_{1N_r} & \cdots & h_{N_t N_r} \end{bmatrix} \text{ and } \mathbf{r} = \begin{bmatrix} r_{1,1} \\ \vdots \\ r_{N_t,1} \end{bmatrix} \quad (7)$$

II.3. General MIMO LP-OFDM transmitter

At the transmit side, MIMO coding and linear precoding are combined in order to exploit the capacity and the diversity of the multi-antenna system. Moreover OFDM modulation is considered to convert the frequency selective MIMO channel into flat fading MIMO channels. Figure 3 depicts the general transmitter scheme of a linearly precoded MIMO-OFDM system including channel coding. A stream of information bits d_n is first encoded and then random

interleaved with Π. These bits are mapped to complex symbols x_k belonging to constellation A by using a Gray mapping. The variance of these symbols is denoted σ_x^2. Successive vectors of L symbols $\mathbf{x} = [x_1 \ \ldots \ x_L]^T$ are linearly precoded by a matrix Θ_L of size $L \times L$ leading to a vector $\mathbf{s} = \Theta_L \mathbf{x}$ of L precoded symbols. Each group of Q symbols is space-time encoded using the coding matrix $\mathbf{S}$. An OFDM modulation is then performed on each sub stream including symbol interleaving, IFFT of size N_{FFT} and cyclic prefix insertion. Finally, the N_t OFDM symbols are sent from a different antenna.

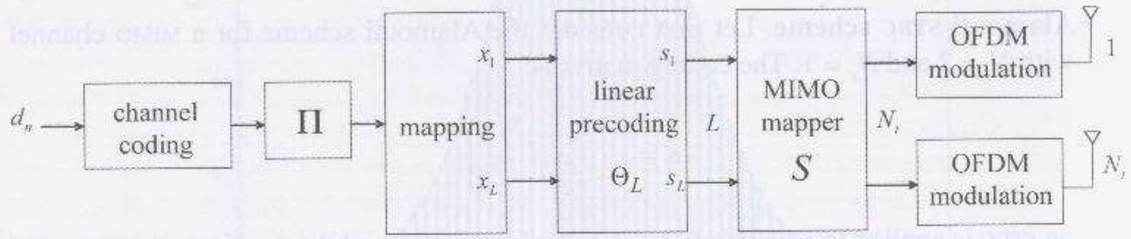

FIG. 3 – General transmitter for LP-OFDM MIMO systems.

Schéma général d'émission de systèmes MIMO OFDM précodés.

II.4. OFDM channel representation

For time-varying and frequency selective MIMO channels, each link from antenna i to antenna j can be modelled by a finite channel impulse response filter of order L_t expressed by:

$$h_t(n) = \sum_{l=0}^{L_t - 1} \alpha_{ij}^{(l)} \delta[n - l] \tag{8}$$

where $\alpha_{ij}^{(l)}$ are time varying channel taps modelled as wide sense stationary random processes. The frequency response of the link can be expressed for each OFDM sub-carrier p as:

$$h_{ij,\,p} = \sum_{l=0}^{L_t - 1} \alpha_{ij}^{(l)} e^{\frac{-j2\pi pl}{N_{FFT}}} \tag{9}$$

The receiver performs OFDM demodulation on each receive antenna by discarding the cyclic prefix to form blocks of N_{FFT} symbols before FFT processing. Under the assumption that the cyclic prefix is well designed, the resulting symbol on subcarrier p and receive antenna j can be written as:

$$r_{j,\,p} = \sum_{j=1}^{N_r} h_{ij,\,p}\, s_{i,\,p} + n_{j,\,p} \qquad p = 1, \ldots, N_{FFT} \tag{10}$$

where $s_{i,\,p}$ is the corresponding symbol sent on subcarrier p and antenna i before OFDM modulation and $n_{j,\,p}$ is the FFT processed additive white Gaussian noise with total variance σ_n^2.

Thus the equivalent channel comprising the OFDM modulators, the MIMO channel and the OFDM demodulators is equivalent to a $N_r \times N_t$ MIMO channel with flat fading per subcarrier as described in Figure 4. With an ideal interleaver in the OFDM process of large size enough and large space between antennas, the $h_{ij,\,p}$ can be considered time, frequency and spatially uncorrelated such that $h_{ij,\,p}$ is i.i.d. zero mean complex Gaussian random sample with unit variance. For brevity, subscript p will be omitted in the following.

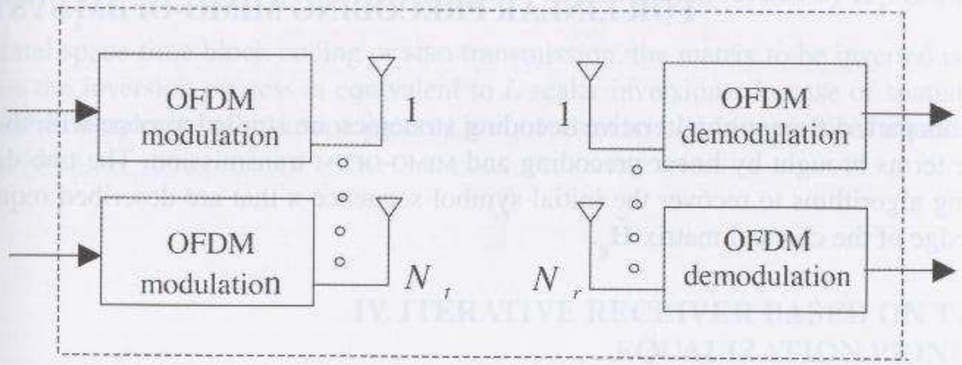

FIG. 4 – OFDM modulation, MIMO channel and OFDM demodulation.

Modulation OFDM, canal MIMO et démodulation OFDM.

II.5. Global channel representation

The extended equivalent matrix $\breve{\mathbf{H}}_g$ of size $\frac{N_r TL}{Q} \times L$ is introduced by including L/Q realizations of equivalent matrix $\breve{\mathbf{H}}$:

$$\breve{\mathbf{H}}_g = diag\ (\underbrace{\ldots,\ \breve{\mathbf{H}},\ldots}_{L/Q}) \tag{11}$$

When applied to precoded symbols, the equivalent representation of the system given by (3) can be rewritten as:

$$\mathbf{y} = \breve{\mathbf{H}}_g\, \Theta_L\, \mathbf{x} + \mathbf{w} \tag{12}$$

where $\mathbf{y}$ is the equivalent receive vector consisting of a stack of L/Q successive vectors $\mathbf{r}$ and $\mathbf{w}$ is the FFT processed additive white Gaussian noise vector with variance $\sigma_w^2 = \sigma_n^2$. Let rewrite $\mathbf{y}$ as a function of the desired symbol x_k :

$$\mathbf{y} = \underbrace{\breve{\mathbf{H}}_g \Theta_L\, \mathbf{e}_k\, x_k}_{\text{desired signal}} + \underbrace{\sum_{n=1,\, n \neq k}^{L} \breve{\mathbf{H}}_g \Theta_L\, \mathbf{e}_n\, x_n}_{\text{IEI terms}} + \underbrace{\mathbf{w}}_{\text{noise term}} \tag{13}$$

where $\mathbf{e}_k$ is a complex vector of size L whose elements are 0 except the k-th element which is 1. The receive signal is corrupted on the one hand by classical Gaussian noise and on the other hand by inter-element interference (IEI) coming from antennas and linear precoding modelled by the off diagonal terms of matrix $\breve{\mathbf{H}}_g \Theta_L$.

III. NON ITERATIVE DECODING STRATEGIES FOR LINEAR PRECODING MIMO-OFDM SYSTEMS

In this part, different non iterative decoding strategies are studied to cope with the interference terms brought by linear precoding and MIMO-OFDM transmission. The two different decoding algorithms to recover the initial symbol sequence $\mathbf{x}$ that are described require the knowledge of the channel matrix $\breve{\mathbf{H}}_g$.

III.1. Maximum likelihood based receiver

Decoding carried out under the Maximum Likelihood criterion consists of searching the sequence $\hat{\mathbf{x}} \in \mathbf{A}^{L\times 1}$ that minimizes the following metric:

$$\hat{\mathbf{x}} = \arg\min_{\mathbf{x}} \| \mathbf{y} - \breve{\mathbf{H}}_g \Theta_L \mathbf{x} \|^2 \tag{14}$$

where $\| . \|^2$ stands for the Frobenius norm. The complexity of such a decoder exponentially grows with the number of antennas, the precoding length and the modulation order. In order to avoid this huge complexity, sphere decoding can be used to decode symbols with a polynomial complexity [7].

III.2. MMSE based equalizer

The transmitted data can also be recovered with a sub-optimal receiver that uses a MMSE criterion based equalizer. Let $\mathbf{w}$ a $L\times 1$ complex equalization vector. The MMSE criterion leads to the following minimization:

$$\mathbf{w}^{opt} = \arg\min_{\mathbf{w}} \mathrm{E}\left[\| \mathbf{x} - \mathbf{w}^H \mathbf{y} \|^2 \right] \tag{15}$$

The Wiener-Hopf solution leads to:

$$\mathbf{w}^{H,\,opt} = \mathbf{e}_k^T \left[\Theta_L^H \breve{\mathbf{H}}_g^H \breve{\mathbf{H}}_g \Theta_L + \frac{\sigma_n^2}{\sigma_x^2} \mathbf{I} \right]^{-1} \Theta_L^H \breve{\mathbf{H}}_g^H \tag{16}$$

where σ_x^2/σ_n^2 represents the average signal-to-noise ratio per antenna and $\mathbf{I}$ a square identity matrix. Since Θ_L is a unitary matrix, then (16) can be rewritten as:

$$\mathbf{w}^{H,\,opt} = \mathbf{e}_k^T \Theta_L^H \left[\breve{\mathbf{H}}_g^H \breve{\mathbf{H}}_g + \frac{\sigma_n^2}{\sigma_x^2} \mathbf{I} \right]^{-1} \breve{\mathbf{H}}_g^H \tag{17}$$

The main complexity of the MMSE equalization comes from the inversion of the matrix $\left[\breve{\mathbf{H}}_g^H \breve{\mathbf{H}}_g + \frac{\sigma_n^2}{\sigma_x^2} \mathbf{I} \right]$ that only depends on the number of antennas modelled by $\breve{\mathbf{H}}_g$. In case of orthogonal space-time block coding or SISO transmission, the matrix to be inverted is diagonal, thus the inversion process is equivalent to L scalar inversions. In case of spatial multiplexing the complexity of inversion process is equivalent to L/N_t inversions of matrices with size $N_t \times N_t$.

IV. ITERATIVE RECEIVER BASED ON TURBO EQUALIZATION PRINCIPLE

In this section, a low complexity iterative receiver is presented where MIMO equalization, linear deprecoding and channel decoding are iteratively processed. Since the receive signal is corrupted by several interference terms (see eq. (13)), a generalized interference canceller can be optimized under MMSE criterion, later called MMSE-IC able to cope with interference terms in a global manner. Two main stages, a LP-MIMO demapper and a Soft-In Soft-Out channel decoder, exchange the information learned from one stage to another iteratively until interference have been cancelled. Each stage is separated from the other one by interleaver or deinterleaver in order to decorrelate data before feeding them to the next stage.

IV.1. General Description

The proposed receiver is depicted in Figure 5. The LP MIMO demapping stage first consists of a MIMO MMSE-IC that removes global interference terms by using *a priori* information of transmitted symbols given by the previous iteration. At first iteration, the LP-MIMO equalizer is reduced to a specific structure that will be later detailed. Equalized symbols $\tilde{x}_k$ are fed to a soft demapper that produces logarithmic likelihood ratio (LLR) $L_{eq}[i, k]$ on coded bits. The channel decoding stage produces improved LLRs $L_{dec}[i, k]$ that are passed via the interleaver Π to the LP-MIMO demapping stage. A soft mapper converts the improved LLRs into estimated symbols $\hat{x}_k$ that are fed again to the MMSE-IC equalizer.

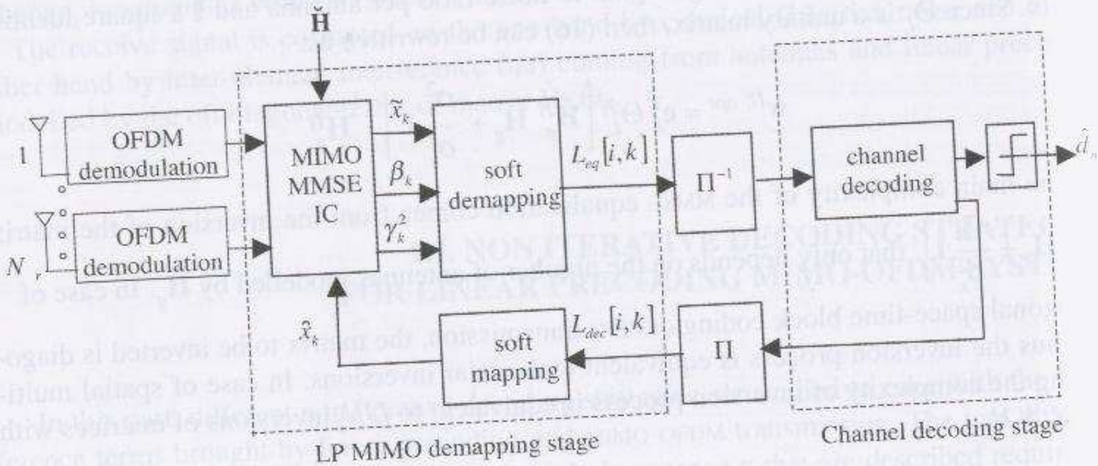

FIG. 5 – Studied iterative receiver.

Récepteur itératif étudié.

IV. 2. Minimum mean square error receiver with *a priori* information

The proposed equalizer structure is based on MMSE soft interference cancellation principle originally introduced in [26] in the field of turbo-equalization for single-carrier transmission. The idea here is to remove the interference terms brought by the linear precoding and the MIMO channel by using soft estimate of transmitted symbols provided by previous iteration. The output of the MMSE-IC can be expressed as:

$$\tilde{x}_k = \mathbf{p}_k^H \mathbf{y} - \mathbf{q}_k^H \hat{\mathbf{a}}_k \tag{18}$$

where $\hat{\mathbf{a}}_k = [\hat{x}_1, \ldots, \hat{x}_{k-1}, 0, \hat{x}_{k+1}, \ldots, \hat{x}_L]^T$ with $\hat{x}_k$ the estimated of x_k given by the previous iteration. The two weight vectors $\mathbf{p}_k$ and $\mathbf{q}_k$ are respectively $\frac{N_r TL}{Q} \times 1$ and $L \times 1$ complex vectors optimized under the MMSE criterion:

$$(\mathbf{p}_k^{opt}, \mathbf{q}_k^{opt}) = \arg \min_{\mathbf{p}_k, \mathbf{q}_k} \mathrm{E}\left[\min_{s \in A_0^i} |x_k - \tilde{x}_k|^2\right] \tag{19}$$

The derivation of the exact equations of the MMSE-IC is presented in Annex B and leads to the following expression:

$$\begin{cases} \mathbf{p}_k^{opt} = \sigma_x^2 \left(\breve{\mathbf{H}}_g \Theta_L \mathbf{V}_k \Theta_L^H \breve{\mathbf{H}}_g^H + \sigma_n^2 \mathbf{I}\right)^{-1} \breve{\mathbf{H}}_g \Theta_L \mathbf{e}_k \\ \mathbf{q}_k^{opt} = \Theta_L^H \breve{\mathbf{H}}_g^H \mathbf{p}_k \end{cases} \tag{20}$$

where

$$\mathbf{V}_k = \sigma_x^2 \mathbf{I} - \sigma_{\hat{x}}^2 \sum_{n=1,\, n \neq k}^{L} \mathbf{e}_n \mathbf{e}_n^T$$

and $\mathbf{I}$ is the $L \times L$ identity matrix whereas $\sigma_{\hat{x}}^2$ is the variance of the estimated symbol $\hat{x}_k$. One can note that a $\frac{N_r TL}{Q} \times \frac{N_r TL}{Q}$ matrix inversion is invoked in order to calculate both optimal weight vectors and this operation is reiterated for each symbol. Let rewrite the expression of $\mathbf{p}_k^{opt}$:

$$\mathbf{p}_k^{opt} = \sigma_x^2 \left(\breve{\mathbf{H}}_g \Theta_L \left[\left(\sigma_x^2 - \sigma_{\hat{x}}^2\right) \mathbf{I} + \sigma_{\hat{x}}^2 \mathbf{e}_k \mathbf{e}_n^H\right] \Theta_L^H \breve{\mathbf{H}}_g^H + \sigma_n^2 \mathbf{I}\right)^{-1} \breve{\mathbf{H}}_g \Theta_L \mathbf{e}_k \tag{21}$$

Invoking the Sherman-Morrison-Woodbury identity $(\mathbf{A} + \mathbf{u}\mathbf{v}^H)^{-1} = \mathbf{A}^{-1} - \frac{\mathbf{A}^{-1}\mathbf{u}\mathbf{v}^H\mathbf{A}^{-1}}{1 + \mathbf{v}^H\mathbf{A}^{-1}\mathbf{u}}$, the latest equation can be expressed as:

$$\mathbf{p}_k^{opt} = \lambda_k \overline{\mathbf{p}}_k^{opt} \tag{22}$$

where

$$\lambda_k = \left[\frac{1}{1 + \sigma_{\hat{x}}^2 \mathbf{e}_k^H \breve{\mathbf{H}}_g^H \overline{\mathbf{p}}_k^{opt}}\right] \tag{23}$$

and

$$\overline{\mathbf{p}}_k^{opt} = \sigma_x^2 \left(\breve{\mathbf{H}}_g \Theta_L \Theta_L^H \breve{\mathbf{H}}_g^H \left(\sigma_x^2 - \sigma_{\hat{x}}^2\right) + \sigma_n^2 \mathbf{I}\right)^{-1} \breve{\mathbf{H}}_g \Theta_L \mathbf{e}_k \tag{24}$$

By using the unitary property of Θ_L, the latest equation can be rewritten as:

$$\overline{\mathbf{p}}_k^{opt} = \sigma_x^2 \left(\breve{\mathbf{H}}_g \breve{\mathbf{H}}_g^H \left(\sigma_x^2 - \sigma_{\hat{x}}^2\right) + \sigma_n^2 \mathbf{I}\right)^{-1} \breve{\mathbf{H}}_g \Theta_L \mathbf{e}_k \tag{25}$$

We can stress on the fact that the previous simplifications lead to relative low complexity: the matrix to be inverted is diagonal per block and only one such inversion is required for a block of L equalized symbols (see section III).

The variance $\sigma_{\hat{x}}^2$ can be simply evaluated by averaging the instantaneous power of the estimated symbols over a sufficient large block of N symbols that usually corresponds to the frame length:

$$\sigma_{\hat{x}}^2 \approx \frac{1}{N} \sum_{k=0}^{N} \left|\hat{x}_k\right|^2 \tag{26}$$

At the first iteration, since no prior information on transmitted symbols is available, a first estimate of transmitted symbols is obtained by setting $\sigma_{\hat{x}}^2 = 0$ and $\hat{\mathbf{a}}_\mathbf{k} = \mathbf{0}$ leading to the classical MMSE equalizer presented in section III:

$$\hat{x}_k^{(1)} = \mathbf{e}_k^T \Theta_L^H \left[\breve{\mathbf{H}}_g^H \breve{\mathbf{H}}_g + \frac{\sigma_n^2}{\sigma_x^2} I\right]^{-1} \breve{\mathbf{H}}_g^H \mathbf{y} \tag{27}$$

where $\hat{x}_k^{(1)}$ stands for estimate of x_k after first iteration.

At the end of the process, the output of the equalizer tends toward the optimal IC structure where $\sigma_{\tilde{x}}^2 = \sigma_x^2$ and $\hat{\mathbf{x}}_\mathbf{k} = \mathbf{x}$ replacing these values in (18), the output of the equalizer becomes exactly equal to the output of a maximum ratio combining (MRC) receiver:

$$\tilde{x}_k = \frac{\sigma_n^2}{\sigma_x^2}\left[\mathbf{e}_k^T \Theta_L^H \breve{\mathbf{H}}_g^H \breve{\mathbf{H}}_g \Theta_L \mathbf{e}_k\right] x_k + \frac{\sigma_n^2}{\sigma_x^2} \mathbf{e}_k^T \Theta_L^H \breve{\mathbf{H}}_g^H \mathbf{n} \tag{28}$$

IV.3. Soft bit mapping/demapping

Equalized symbols are first converted to LLR on coded bits. Under the assumption that the output of the equalizer follows a Gaussian law and according to the "max-log" approximation, the LLR on the i-th coded bit of the k-th demapped symbol can be expressed as:

$$L_{eq}[i, k] = \frac{1}{2\gamma_k^2}\left[\min_{s \in A_0^i} \left|\tilde{s}_k - \beta_k s\right|^2 - \min_{s \in A_1^i} \left|\tilde{s}_k - \beta_k s\right|^2\right] \tag{29}$$

where A_b^i denotes the subset of the constellation for which i-th bit is equal to b whereas β_k and γ_k^2 denote the bias at the output of the equalizer and the variance of the noise plus interference terms respectively. These values are derived from Eq. (13) and (18):

$$\beta_k = \mathbf{p}_k^H \breve{\mathbf{H}}_g \Theta_L \mathbf{e}_k \tag{30}$$

$$\gamma_k^2 = \sigma_s^2 \beta_k (1 - \beta_k) \tag{31}$$

The soft mapper provides the inverse transformation at the output of the channel decoder by converting the block of $[L_{dec}[1, k], \ldots, L_{dec}[\mathbf{m}, k]]$ calculated by the decoder into a soft symbol $\hat{x}_k$. If we denote $[b_1 \ldots b_m]$ the bits that constitute the m-ary symbol belonging to constellation A, the soft estimated symbol is given by the following expression [27]:

$$\hat{x}_k = \sum_{x \in A} x \prod_{i=1}^{m}\left[\frac{1}{2} + \frac{2b^i - 1}{2} \tanh\left(\frac{L_{dec}(i, k)}{2}\right)\right] \tag{32}$$

IV.4. Channel decoding

The input of the channel decoding stage is the set of *a priori* LLRs of coded bits. The channel decoder processes the soft information, computes refined LLRs of coded bits and at the last iteration the LLR of the information bits. A forward-backward algorithm of the type of BCJR [32] could be implemented here. For complexity reason, we prefer using the soft output Viterbi algorithm (SOVA) that provides only slight performance degradation [33].

V. SIMULATION RESULTS

Simulations have been carried out with a half rate convolutional code with $(133, 177)_o$ as generator polynomials and a QPSK modulation leading to a raw spectral efficiency of $\eta = \frac{Q}{T}$ bps/Hz. All system parameters are presented in Table I. The following power normalization is assumed:

$$\mathrm{E}\left[\left|x_k\right|^2\right] = \sigma_x^2 = \frac{1}{N_t N_r} \tag{33}$$

Thus, results do not include additional array gain. The channel model is chosen Rayleigh i.i.d. modelling an ideal OFDM transmission over time and frequency channel. This assumption can be easily verified by carefully designing in the OFDM process the guard interval, the inter-carrier spacing and the interleaving depth according to the time and frequency coherence of the channel. Furthermore, sufficient spacing between transmit and receive antennas is assumed leading to a perfect uncorrelation between each link. Degradation due to correlation between antennas is not evaluated here but would probably remains low as demonstrated in [21] for spatial multiplexing scheme including similar iterative receiver. In fact for a theoretical correlation of 30%, degradation in bit error rate is inferior to 1 dB at 10^{-4}. Finally, we assume that perfect channel information is available on the receiver side. This can be accomplished by classical means of channel estimation, e.g. insertion of pilot symbols or pilot tones.

TABLE I. – Main system parameters.

Principaux paramètres système.

	set A	set B	set C
Channel coding	1/2 rate NRSC (133, 171)o		
Bit interleaver	Random type, 10000 bits		
Constellation	QPSK		
Linear precoding matrix	Hadamard complex		
Linear precoding size	none, 4, 8, 16 or 64		
Antenna configuration	1×1	2×1	2×2
Space-time mapping	none	Alamouti	Spatial multiplexing
Raw spectral efficiency n	1 bps/Hz	1 bps/Hz	2 bps/Hz

V.1. SISO transmission

In Figure 6 and Figure 7, bit error rate performance (BER) is presented in case of SISO transmission, that is one transmit antenna and one receive antenna. Figure 6 provides performance results of the MMSE non-iterative receiver for different precoding sizes. For compari-

son, we add the curve labelled 'no LP' that corresponds to a system where no linear precoding has been implemented thus performance provided are those of an OFDM system with a classical ZF equalization. As demonstrated in [8], we can note that LP-OFDM outperforms OFDM if the SNR is greater than a threshold that depends on the channel code structure and the precoding length. In case of the half rate convolutional code, this threshold is equal to 3.5 dB, 4.5 dB and 6 dB for $L = 4$, $L = 8$ and $L = 64$ respectively. The degradation of LP-OFDM compared to OFDM is due to interference terms brought by the linear precoding. By increasing the precoding size, the asymptotical performance of LP-OFDM are improved owing to a better exploitation of the signal-space diversity but the degradation due to interference terms becomes slightly greater at low SNR. Same performance results have been obtained for $L = 16$ and $L = 64$. Therefore following simulations are carried out with $L = 16$.

Figure 7 provides the performance of the proposed iterative receiver. Interference terms are progressively removed during the iterative process leading to meaningful gains after only a few iterations. At BER = 10^{-4} the gain over the non-precoded curve is about 2.5 – 3.5 dB depending on the size of L. For $L = 16$, Gaussian curve is reached for Eb/N0 > 3 dB, meaning that signal space and code diversities are fully exploited. Only 4 iterations are required to reach these performances. Same results have been obtained in [23].

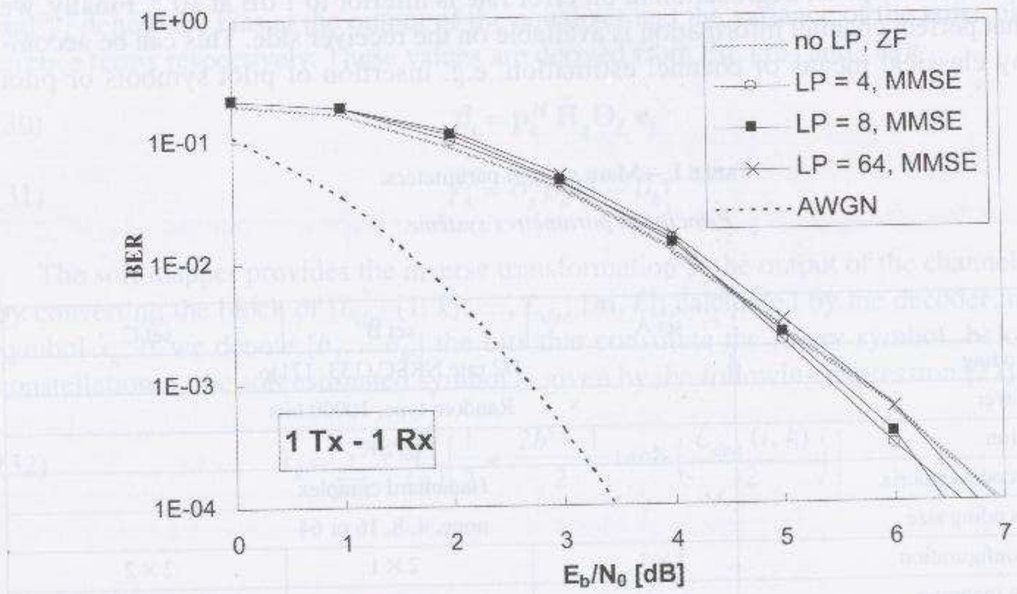

FIG. 6 – Performance of the MMSE non-iterative receiver for a LP scheme over a SISO Rayleigh fading channel, with a QPSK and $\eta = 1$ bps/Hz.

Performance d'un récepteur MMSE non itératif pour un schéma avec du précodage linéaire sur canal SISO à évanouissement de type Rayleigh, une modulation QPSK et $\eta = 1$ bit/(s.Hz).

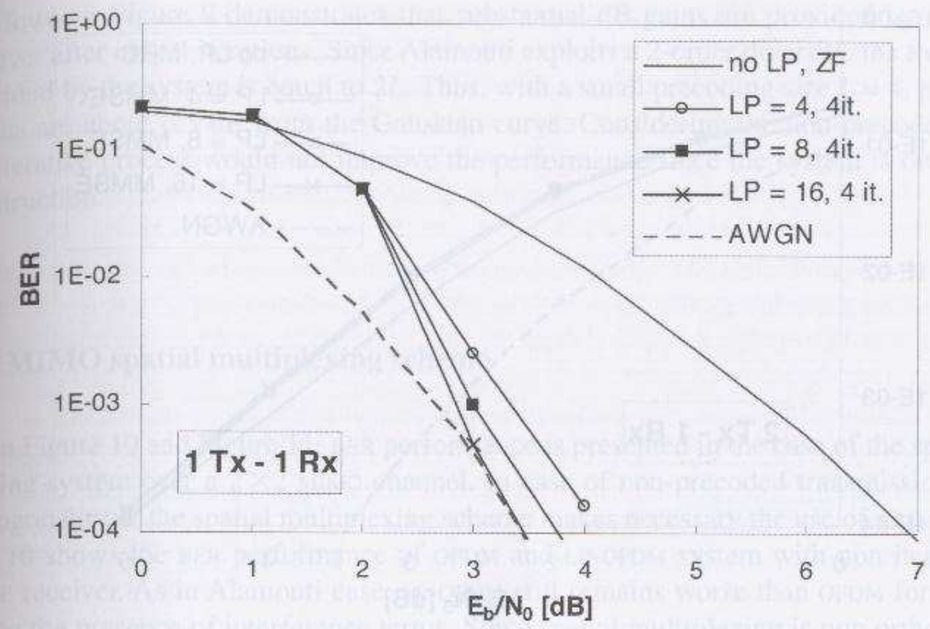

FIG. 7 – Performance of the proposed iterative receiver with 4 iterations for a LP scheme over a SISO Rayleigh fading channel, with QPSK and $\eta = 1$ bps/Hz.

Performance du récepteur itératif proposé après 4 itérations pour un schéma avec du précodage linéaire sur un canal SISO à évanouissement de type Rayleigh, une modulation QPSK et $\eta = 1$ bit/(s.Hz).

V.2. MIMO STBC scheme

Figure 8 and Figure 9 present BER performance in case of Alamouti STBC scheme over a MIMO channel. Performance results of the non-iterative receiver are shown in Figure 8. Since the Alamouti code is orthogonal, the classical MRC receiver is used for the non-precoded system. However by adding precoding, the resulting system becomes non-orthogonal and thus the MMSE linear receiver is considered. We can notice that the SNR threshold for which LP-OFDM outperforms the OFDM curve is quite higher than in SISO case. In fact the intersection point is located at Eb/N0 ≈ 5 dB. This can be explained by the fact that the Alamouti code with no precoding provides a 2-order diversity without bringing interference terms. The additional diversity brought by the linear precoding is negligible comparatively to the number of interference terms created.

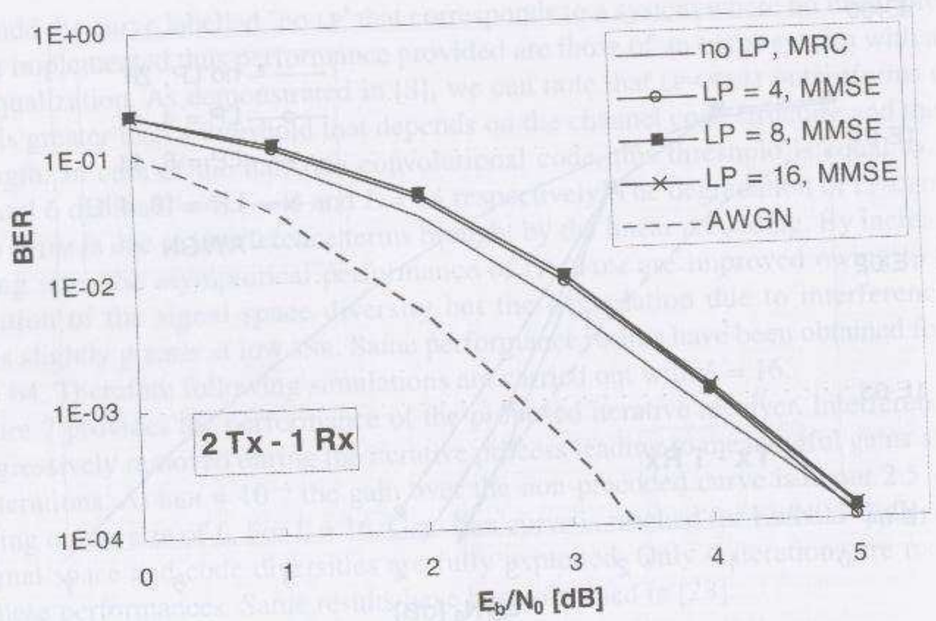

FIG. 8 – Performance of the MMSE non-iterative receiver for a LP Alamouti over a 2×1 Rayleigh fading channel, with QPSK, and $\eta = 1$ bps/Hz.

Performance d'un récepteur MMSE non itératif pour un schéma avec un codage espace temps d'Alamouti et du précodage linéaire sur un canal MIMO 2×1 à évanouissements de type Rayleigh, une modulation QPSK et $\eta = 1$ bit/(s.Hz).

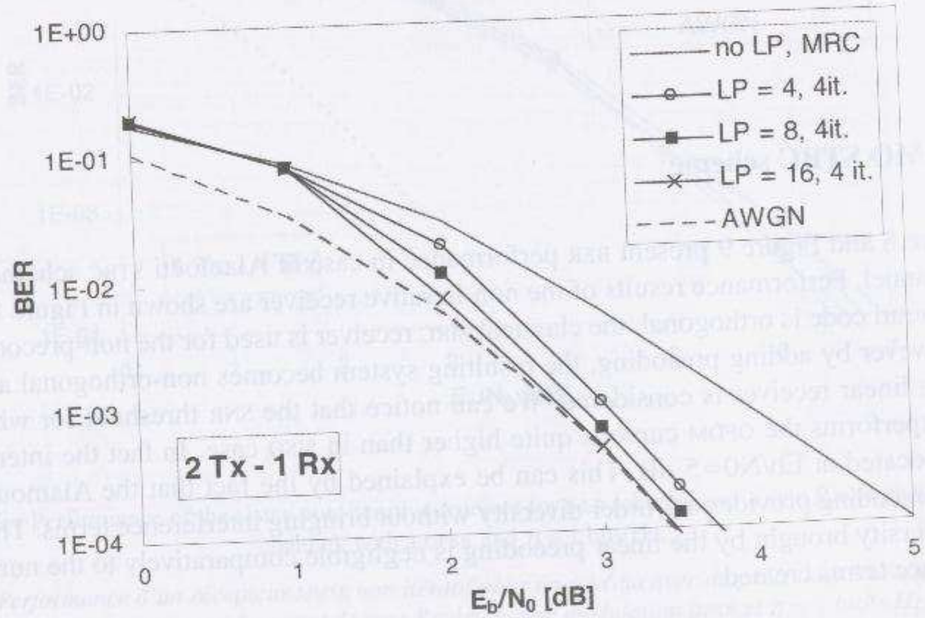

FIG. 9 – Performance of the proposed iterative receiver with 4 iterations for a LP Alamouti scheme over a 2×1 Rayleigh fading channel, with QPSK and $\eta = 1$ bps/Hz.

Performance d'un récepteur itératif pour un schéma avec un codage espace temps d'Alamouti et du précodage linéaire sur un canal MIMO 2×1 à évanouissement de type Rayleigh, une modulation QPSK et $\eta = 1$ bit/(s.Hz).

However Figure 9 demonstrates that substantial dB gains are provided by the iterative receiver after only 4 iterations. Since Alamouti exploits a 2-order diversity, the total diversity provided by the system is equal to $2L$. Thus, with a small precoding size $L = 4$, performance results are about 0.5 dB from the Gaussian curve. Considering the non-precoded scenario, the iterative process would not improve the performance since the system is orthogonal by construction.

V.3. MIMO spatial multiplexing scheme

In Figure 10 and Figure 11, BER performance is presented in the case of the spatial multiplexing system over a 2×2 MIMO channel. In case of non-precoded transmission, the non-orthogonality of the spatial multiplexing scheme makes necessary the use of a MMSE receiver. Fig. 10 shows the BER performance of OFDM and LP-OFDM system with non iterative linear MMSE receiver. As in Alamouti case, LP-OFDM still remains worse than OFDM for BER $> 10^{-4}$ due to the presence of interference terms. Since spatial multiplexing is non orthogonal, performance results remain inferior to the Alamouti one at same power per receive antenna thus without taking into account the 3 dB receive antenna gain of the 2×2 scheme.

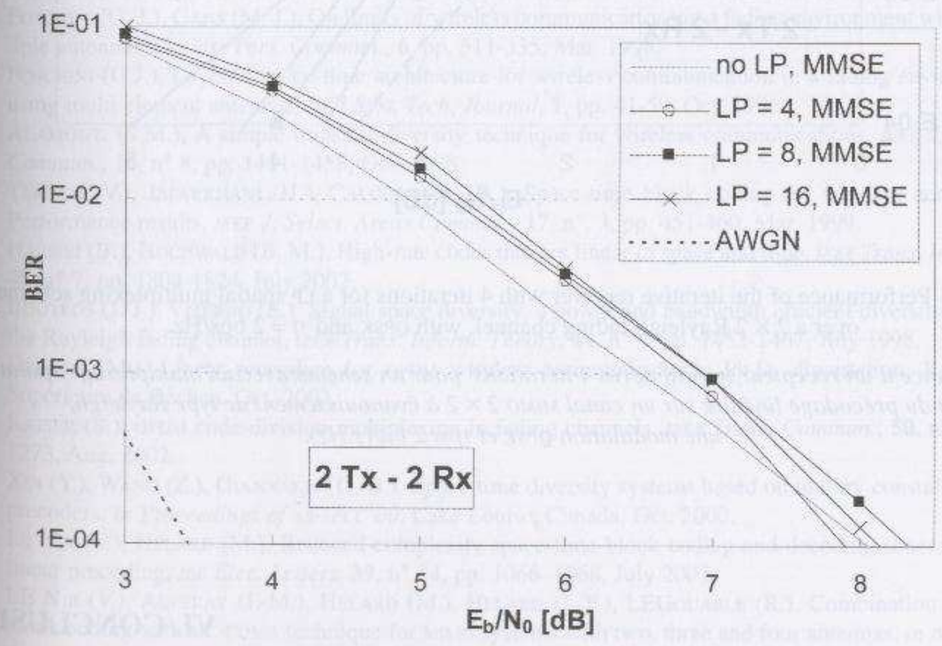

FIG. 10 – Performance of the MMSE non-iterative receiver for a LP spatial multiplexing scheme over a 2×2 Rayleigh fading channel, with QPSK and $\eta = 2$ bps/Hz.

Performance d'un récepteur MMSE non-itératif pour un schéma avec un multiplexage spatial et du précodage linéaire sur un canal MIMO 2×2 à évanouissement de type Rayleigh, une modulation QPSK et $\eta = 2$ bit/(s.Hz).

Performance results with the proposed iterative receiver are presented in Figure 11. Since OFDM and LP-OFDM system are both non-orthogonal in case of spatial multiplexing, the proposed iterative receiver is used for the two cases. Please note that the iterative receiver for the non precoded scenario has already been proposed in [19]. By using linear precoding, an extra gain of 0.8 – 1.3 dB gain at BER = 10^{-4} is won over the spatial multiplexed OFDM. This can be explained by the fact that linear precoding systems exploit higher orders of diversity than the classical OFDM.

As for Alamouti case, with $L = 16$, Gaussian performance are reached at a higher SNR. but this a double spectral efficiency.

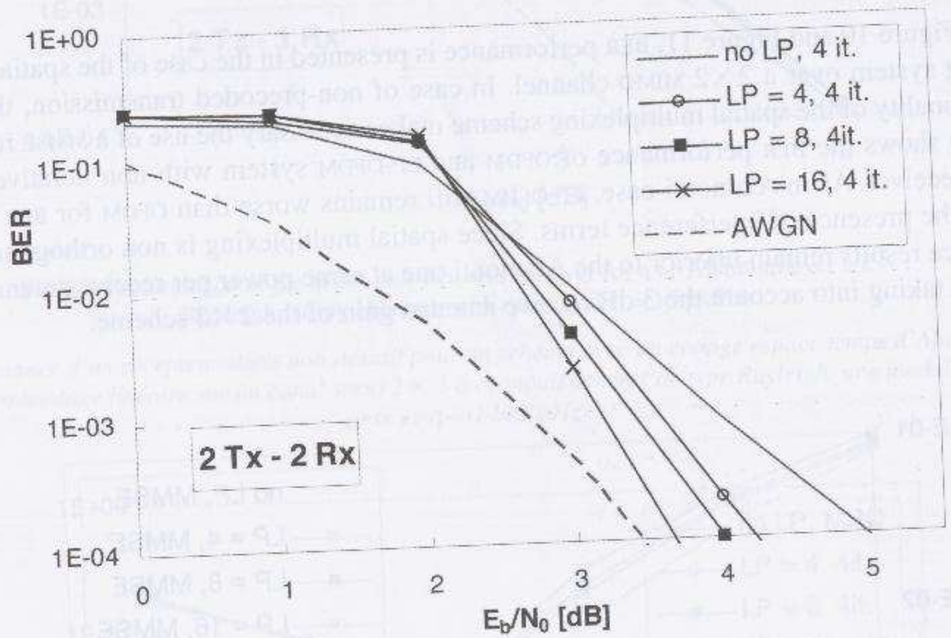

FIG. 11 – Performance of the iterative receiver with 4 iterations for a LP spatial multiplexing scheme over a 2×2 Rayleigh fading channel, with QPSK and $\eta = 2$ bps/Hz.

Performance d'un récepteur itératif après 4 itérations pour un schéma avec un multiplexage spatial et du précodage linéaire sur un canal MIMO 2×2 à évanouissement de type Rayleigh, une modulation QPSK et $\eta = 2$ bit/(s.Hz).

VI. CONCLUSION

In this paper, an efficient iterative receiver is performed for LP-OFDM systems in SISO and MIMO transmissions. By iteratively removing global interference terms brought by the transmitter and the MIMO channel, the proposed receiver tends toward the optimal curve given by the coded Gaussian curve with only a few number of iterations demonstrating that frequency, time and signal space diversities are efficiently exploited. Since the equalization stage inside

the iterative process only requires matrix operations depending on the MIMO architecture, th receiver leads to a lower complexity than ML based solutions described in state of the ar Thus, large size of precoding matrix, high order modulation and high number of antenna can be used while keeping feasible algorithm at the receive side. The proposed receiver ca easily be adapted to other MIMO transmission schemes by matching the equivalent matrix $\breve{\mathbf{H}}$ t the desired space-time coding.

Under theoretical uncorrelated channels, all studied systems converge toward the sam asymptotical performance with the proposed iterative process. Nevertheless, with i "double" capacity, the spatial multiplexing system outperforms the other ones. Taking int account correlation between antennas should slightly degrade BER performance as noted i similar MIMO systems without linear precoding. In order to compare different system receive antenna gain and the addressed spectral efficiency should of course be taken int account as well as different spatial, time and frequency diversities available in the channel.

Manuscrit reçu le 30 juin 200
Accepté le 8 mars 200

REFERENCE

[1] TELATAR (E.), Capacity of multi-antenna gaussian channel, *Bell Labs. Tech. Memo.*, June 1995.
[2] FOSCHINI (G. J.), GANS (M. J.), On limits of wireless communications in a fading environment when using mu tiple antenna, *Wireless Pers. Commun.*, **6**, pp. 311-335, Mar. 1998.
[3] FOSCHINI (G.J.), Layered space-time architecture for wireless communication in a fading environment whe using multi element antennas, *Bell Syst. Tech. Journal*, **1**, pp. 41-59, Oct. 1996.
[4] ALAMOUTI (S.M.), A simple transmit diversity technique for wireless communications, *IEEE J. Select. Are Commun.*, **16**, n° 8, pp. 1451-1458, Oct. 1998.
[5] TAROKH (V.), JAFARKHANI (H.), CALDERBANK (R.), Space-time block coding for wireless communication Performance results, *IEEE J. Select. Areas Commun.*, **17**, n°. 3, pp. 451-460, Mar. 1999.
[6] HASSIBI (B.), HOCHWALD (B. M.), High-rate codes that are linear in space and time, *IEEE Trans. Inform. Theor* **48**, n° 7, pp. 1804-1824, July 2002.
[7] BOUTROS (J. J.), VITERBO (E.), Signal space diversity: a power and bandwidth efficient diversity technique f the Rayleigh fading channel, *IEEE Trans. Inform. Theory*, **44**, n° 4, pp. 1453-1467, July 1998.
[8] DEBBAH (M.), Linear precoders for OFDM wireless communications, Ph.D. dissertation, Ecole nationa Supérieure de Cachan, Oct. 2002.
[9] KAISER (S.), OFDM code-division multiplexing in fading channels, *IEEE Trans. Commun.*, **50**, n° 8, pp. 126 1273, Aug. 2002.
[10] XIN (Y.), WANG (Z.), GIANNAKIS (G. B.), Space-time diversity systems based on unitary constellation-rotatin precoders, *in Proceedings of AS-SPCC'00*, Lake Louise, Canada, Oct. 2000.
[11] LE NIR (V.), HELARD (M.), Reduced-complexity space-time block coding and decoding schemes with bloc linear precoding, *IEE Elec. Letters*, **39**, n° 14, pp. 1066–1068, July 2003.
[12] LE NIR (V.), AUFFRAY (J.-M.), HELARD (M.), HELARD (J.-F.), LEGOUABLE (R.), Combination of space-tim block coding with MC-CDMA technique for MIMO systems with two, three and four antennas, *in IST Summit '0* Aveiro, Portugal, June 2003.
[13] DAMEN (M. O.), BEAULIEU (N.C.), On diagonal algebraic space-time block codes, *IEEE Trans. Inform. Theor* **51**, n° 6, pp. 911-919, June 2003.
[14] MA (X.), GIANNAKIS (G.B.), Full-diversity full-rate complex-field space-time coding, *IEEE Trans. Signa Processing*, **51**, n° 11, pp. 2917-2930, 2003.
[15] DOUILLARD (C.), PICART (A.), DIDIER (P.), JEZEQUEL (M.), BERROU (C.), GLAVIEUX (A.), Iterative correction intersymbol interference: Turbo-equalization, *Eur. Trans. Telecommunications*, **6,** n° 5, Sept. 1995.
[16] WANG (Z.), ZHOU (S.), GIANNAKIS (G.B.), Joint coding-precoding with low-complexity turbo-decoding, *IE Trans. Commun.*, **3**, n° 3, pp. 832-842, May 2004.

[17] TONELLO (A. M.), Space-time bit-interleaved coded modulation with an iterative decoding strategy, *in Proceedings of VTC Fall'00*, Boston, USA, pp. 473-478, Sept.2000.
[18] BOUTROS (J J.), GRESSET (N.), BRUNEL (L.), Turbo coding and decoding for multiple antenna channels, *in Proceedings of ISTC'03*, Brest, France, Sept. 2003.
[19] SELLATHURAI (M.), HAYKIN (S.), TURBO-BLAST for wireless communications: theory and experiments, *IEEE Trans. Signal Processing*, **50**, n° 10, pp. 2538-2546, Oct. 2002.
[20] BOUVET (P.-J.), HELARD (M.), LE NIR (V.), Low complexity iterative receiver for non-orthogonal space-time block code with channel coding, *in Proceedings of VTC Fall '04*, Los Angeles, USA, Sept. 2004.
[21] BOUVET (P.-J.), HELARD (M.), Efficient iterative receiver for spatial multiplexed OFDM system over time and frequency selective channels, *in Proceedings of World Wireless Conference 2005*, San Francisco Bay area, USA, May 2005.
[22] WITZKE (M.), Linear and widely linear filtering applied to iterative detection of generalized MIMO signals, *Annals of Telecommunications*, **60**, n° 1-2, pp. 147-168, January-February 2005.
[23] BOUVET (P.-J.), LE NIR (V.), HELARD (M.), Low complexity iterative receiver for linear precoded OFDM", *in Proceedings of WIMOB'05*, Montreal, Canada, Aug. 2005.
[24] LE MASSON (J.), LANGLAIS (C.), BERROU (C.), Linear precoding with low complexity MMSE turbo-equalization and application to the wireless LAN system, *in Proceedings of ICC'05*, Seoul, Korea, May 2005.
[25] REYNOLDS (D.), WANG (X.), Low complexity turbo-equalization for diversity channels, *Signal Processing*, **85**, n° 5, pp. 989-995, May 2001.
[26] TÜCHLER (M.), KOETTER (R.), SINGER (A. C.), Minimum mean squared error equalization using *a priori* information, *IEEE Trans. Signal Processing*, **50**, n° 3, pp. 673-683, Mar. 2002.
[27] LAOT (C.), LE BIDAN (R.) LEROUX (D.), Low complexity linear turbo equalization: A possible solution for EDGE, *IEEE Trans. Wireless. Commun.*, **4**, n° 3, May 2005.
[28] BOUVET (P.-J.), HELARD (M.), LE NIR (V.), Low complexity iterative receiver for linear precoded MIMO systems, *in Proceedings of ISSSTA'04*, Sydney, Australia, Aug. 2004.
[29] OMORI (H.), ASAI (T.), MATSUMOTO (T.), A matched filter approximation for sc/mmse iterative equalizers, *IEEE Commun. Lett.*, **5**, pp. 310–312, 2001.
[30] XIN (Y.), WANG (Z.), GIANNAKIS (G. B.), Space-time constellation-rotating codes maximizing diversity and coding gains, *in Proceedings of GLOBECOM'01*, San Antonio, Texas, Nov. 2001.
[31] SHANNON (C. E.), Communication in the presence of noise, *IRE Trans. Inform.Theory*, **37**, pp. 10-21, 1949.
[32] BAHL (L.), COCKE (J.), JELINECK (F.), RAVIV (J.), Optimal decoding of linear codes for minimizing symbol error rate, *IEEE Trans. Inform. Theory*, **20**, n° 3, pp. 284-287, Mar. 1974.
[33] BERROU (C.), ADDE (P.), ANGUI (E.), FAUDEIL (S.), A low complexity soft-output Viterbi decoder architecture, *in Proceedings of ICC'93*, Geneva, Switzerland, May 1993, pp. 737-740.

Annexe A

In this Annex, the unitary linear precoding matrices described are the Fourier, the Vandermonde and the complex Hadamard matrices of size $L \times L$.

A. Fourier matrices

$$\Theta_L^{FFT} = \frac{1}{\sqrt{L}} \begin{bmatrix} 1 & 1 & 1 & \cdots & 1 \\ 1 & w^1 & w^2 & \cdots & w^{L-1} \\ 1 & w^2 & w^4 & \cdots & w^{2(L-1)} \\ \vdots & \vdots & \vdots & \ddots & \vdots \\ 1 & w^{L-1} & w^{2(L-1)} & \cdots & w^{(L-1)(L-1)} \end{bmatrix} \quad (34)$$

with $w = e^{\frac{j2\pi}{L}}$.

B. Vandermonde matrices

$$\Theta_L^{Van} = \mathrm{diag}\left[1, \alpha, \alpha^2, \ldots, \alpha^{L-1}\right] \Theta_L^{FFT} \quad (35)$$

$$\Theta_L^{Van} = \frac{1}{\sqrt{L}} \begin{bmatrix} 1 & 1 & 1 & \cdots & 1 \\ \theta_1 & \theta_2 & \theta_3 & \cdots & \theta_{L-1} \\ \theta_1^2 & \theta_2^2 & \theta_3^2 & \cdots & \theta_{(L-1)}^2 \\ \vdots & \vdots & \vdots & \ddots & \vdots \\ \theta_1^{L-1} & \theta_2^{L-1} & \theta_3^{L-1} & \cdots & \theta_{(L-1)}^{(L-1)} \end{bmatrix} \quad (36)$$

with $\theta_i = \alpha w^i = \beta e^{2ij\pi}$.

C. Complex Hadamard matrices based on SU(2) group

$$\Theta_L^{Had} = \sqrt{\frac{2}{L}} \begin{bmatrix} \Theta_{L/2} & \Theta_{L/2} \\ \Theta_{L/2} & -\Theta_{L/2} \end{bmatrix} \quad (37)$$

with $L = 2^n$, $n \geq 2$ and

$$\Theta_2 = \begin{bmatrix} e^{j\theta_1}.\cos\eta & e^{j\theta_2}.\sin\eta \\ -e^{j\theta_2}.\sin\eta & e^{j\theta_1}.\cos\eta \end{bmatrix} \quad (38)$$

belonging to the Special Unitary group SU(2), therefore $\det(\Theta_2) = 1$ and $\Theta_2^{-1} = \Theta_2^H$.

Annexe B

In this annex, we derive the equation of the proposed MMSE Interference Canceller presented in section IV. The optimum filters are solution of the following optimization problem:

$$(\mathbf{p}_k^{opt}, \mathbf{q}_k^{opt}) = \arg \min_{\mathbf{p}_k, \mathbf{q}_k} \mathrm{E}\left[\left| x_k - \tilde{x}_k \right|^2\right] \tag{39}$$

The optimum weight vectors $\mathbf{p}_k^H$ and $\mathbf{q}_k^H$ are determined in two steps. We begin by developing the expression of the signal to interference and noise ratio (SINR). Let rewrite the expression of the equalized symbol as a function of x_k :

$$\tilde{x}_k = \underbrace{\mathbf{p}_k^H \breve{\mathbf{H}}_g \Theta_L \mathbf{e}_k x_k}_{\text{useful term}} + \underbrace{\mathbf{p}_k^H \breve{\mathbf{H}}_g \Theta_L \mathbf{a}_k - \mathbf{q}_k^H \hat{\mathbf{a}}_k}_{\text{IEI terms}} + \underbrace{\mathbf{p}_k^H \mathbf{n}}_{\text{noise term}} \tag{40}$$

where $\mathbf{e}_k$ is a vector of length L whose elements are 0 except the k-th element which is 1. The expression of the SINR is:

$$\text{SINR} = \frac{\mathrm{E}[\mathbf{p}_k^H \breve{\mathbf{H}}_g \Theta_L \mathbf{e}_k \mathbf{e}_k^H \Theta_L^H \breve{\mathbf{H}}_g^H \mathbf{p}_k]. \sigma_x^2}{\mathrm{E}[(\mathbf{p}_k^H \breve{\mathbf{H}}_g \Theta_L \mathbf{a}_{k_k} - \mathbf{q}_k^H \hat{\mathbf{a}}_k + \mathbf{p}_k^H \mathbf{n}).(\mathbf{p}_k^H \breve{\mathbf{H}}_g \Theta_L \mathbf{a}_{k_k} - \mathbf{q}_k^H \hat{\mathbf{a}}_k + \mathbf{p}_k^H \mathbf{n})^H]} = \frac{\sigma_U^2}{\sigma_{NI}^2} \tag{41}$$

Following [26], we propose to determine the optimum filter which maximizes the SINR at the equalizer output. In fact, the max-SNR criterion constitutes a generalization of the standard MMSE criterion. By looking at the SINR expression, we can notice that only the denominator depends on $\mathbf{q}_k$, thus the optimal weight vector $\mathbf{q}_k^{opt}$ can be determined by minimizing the term σ_{NI}^2. By deriving with respect to $\mathbf{q}_k$ we obtain:

$$\frac{\partial \sigma_{NI}^2}{\partial \mathbf{q}_k} = -\mathrm{E}\left[\hat{\mathbf{a}}_k \mathbf{a}_k^H\right] \Theta_L^H \breve{\mathbf{H}}_g^H \mathbf{p}_k - \mathrm{E}\left[\hat{\mathbf{a}}_k \mathbf{n}^H\right] \mathbf{p}_k + \mathrm{E}\left[\hat{\mathbf{a}}_k \mathbf{a}_k^H\right] \mathbf{q}_k \tag{42}$$

One can demonstrate that $\mathrm{E}\left[\hat{\mathbf{a}}_k \mathbf{a}_k^H\right] = \mathrm{E}\left[\hat{\mathbf{a}}_k \hat{\mathbf{a}}_k^H\right]$. Moreover we assume a perfect non correlation between symbols and noise.

By setting $\frac{\partial \sigma_{NI}^2}{\partial \mathbf{q}_k} = 0$ we found the first optimal weight vector:

$$\mathbf{p}_k^{opt} = \Theta_L^H \breve{\mathbf{H}}_g^H \mathbf{p}_k \tag{43}$$

The expression of the equalized symbol becomes:

$$\begin{aligned} \tilde{x}_k &= \mathbf{p}_k^H \mathbf{y} - \mathbf{p}_k^H \breve{\mathbf{H}}_g \Theta_L \hat{\mathbf{a}}_k + \mathbf{p}_k^H \mathbf{n} \\ \tilde{x}_k &= \mathbf{p}_k^H (\mathbf{y} - \breve{\mathbf{H}}_g \Theta_L \hat{\mathbf{a}}_k) + \mathbf{p}_k^H \mathbf{n} \end{aligned} \tag{44}$$

and new expression of the MSE is:

$$\varepsilon_k^2 \overset{\Delta}{=} \mathrm{E}\left[(x_k - \mathbf{p}_k^H (\mathbf{y} - \breve{\mathbf{H}}_g \Theta_L \hat{\mathbf{a}}_k))\ (x_k - \mathbf{p}_k^H (\mathbf{y} - \breve{\mathbf{H}}_g \Theta_L \hat{\mathbf{a}}_k))^H\right] \tag{45}$$

Let derive with respect to $\mathbf{p}_k$:

$$\frac{\partial \varepsilon_k^2}{\partial \mathbf{p}_k} = \mathrm{E}\left[\underbrace{(\mathbf{y} - \breve{\mathbf{H}}_g \Theta_L \hat{\mathbf{a}}_k)\ (\mathbf{y} - \breve{\mathbf{H}}_g \Theta_L \hat{\mathbf{a}}_k)^H}_{\mathrm{R}}\right] \mathbf{p}_k - \mathrm{E}\left[\underbrace{(\mathbf{y} - \breve{\mathbf{H}}_g \Theta_L \hat{\mathbf{a}}_k)}_{u} x_k^*\right] \tag{46}$$

By setting $\frac{\partial \sigma_{NI}^2}{\partial \mathbf{q}_k} = 0$, we obtain:

$$\mathbf{p}_k^{opt} = \mathbf{R}^{-1} \mathbf{u} \tag{47}$$

By assuming perfect uncorrelation between two different symbols, we have:

$$\begin{aligned} \mathbf{R} &= \breve{\mathbf{H}}_g \Theta_L \mathrm{E}[(x_k - \hat{a}_k).(x_k - \hat{a}_k)^H]\ \Theta_L^H \breve{\mathbf{H}}_g^H + \mathrm{E}[\mathbf{n}\mathbf{n}^H)] \\ &= \breve{\mathbf{H}}_g \Theta_L \left(\mathrm{E}[\mathbf{x}\mathbf{x}^H] - \mathrm{E}[\hat{\mathbf{a}}_k \hat{\mathbf{a}}_k^H]\right) \Theta_L^H \breve{\mathbf{H}}_g^H + \sigma_n^2 \mathbf{I} \\ &= \breve{\mathbf{H}}_g \Theta_L \mathbf{V}_k \Theta_L^H \breve{\mathbf{H}}_g^H + \sigma_n^2 \mathbf{I} \end{aligned} \tag{48}$$

where $\mathbf{V}_k = diag\ [\sigma_x^2 - \sigma_{\hat{x}}^2, \ldots, \sigma_x^2, \ldots, \sigma_x^2 - \sigma_{\hat{x}}^2]$ is a complex matrix of size $L \times L$ which is the covariance matrix of $\mathbf{x} - \hat{\mathbf{x}}$ where the k-th element of the diagonal is set to σ_x^2 and where $\sigma_{\hat{x}}^2$ is the variance of the estimated symbols. On the other hand we have:

$$\mathbf{u} = \breve{\mathbf{H}}_g \Theta_L \mathrm{E}[(\mathbf{x} x_k^*] = \sigma_x^2 \breve{\mathbf{H}}_g \Theta_L \mathbf{e}_k \tag{49}$$

Thus, the final expression of the optimal weight vector is:

$$\mathbf{p}_k^{opt} = \sigma_x^2 (\breve{\mathbf{H}}_g \Theta_L \mathbf{V}_k \Theta_L^H \mathbf{H}_g^H + \sigma_n^2 \mathbf{I})^{-1} \breve{\mathbf{H}}_g \Theta_L \mathbf{e}_k \tag{50}$$